JCTC Journal of Chemical Theory and Computation

ARTICLE

pubs.acs.org/JCTC

Variational Monte Carlo Method with Dirichlet Boundary Conditions: Application to the Study of Confined Systems by Impenetrable Surfaces with Different Symmetries

Antonio Sarsa*,† and Claude Le Sech‡

†Departmento de Física, Campus de Rabanales Edif. C2, Universidad de Córdoba, E-14071 Córdoba, Spain

‡Institut des Sciences Moleculaires d'Orsay-ISMO (UMR 8214), Université Paris Sud 11, CNRS, 91405, Orsay Cedex, France

ABSTRACT: Variational Monte Carlo method is a powerful tool to determine approximate wave functions of atoms, molecules, and solids up to relatively large systems. In the present work, we extend the variational Monte Carlo approach to study confined systems. Important properties of the atoms, such as the spatial distribution of the electronic charge, the energy levels, or the filling of electronic shells, are modified under confinement. An expression of the energy very similar to the estimator used for free systems is derived. This opens the possibility to study confined systems with little changes in the solution of the corresponding free systems. This is illustrated by the study of helium atom in its ground state ^{1}S and the first ^{3}S excited state confined by spherical, cylindrical, and plane impenetrable surfaces. The average interelectronic distances are also calculated. They decrease in general when the confinement is stronger; however, it is seen that they present a minimum for excited states under confinement by open surfaces (cylindrical, planes) around the radii values corresponding to ionization. The ground ^{2}S and the first ^{2}P and ^{2}D excited states of the lithium atom are calculated under spherical constraints for different confinement radii. A crossing between the ^{2}S and ^{2}P states is observed around $r_c = 3$ atomic units, illustrating the modification of the atomic energy level under confinement. Finally the carbon atom is studied in the spherical symmetry by using both variational and diffusion Monte Carlo methods. It is shown that the hybridized state sp^3 becomes lower in energy than the ground state ^{3}P due to a modification and a mixing of the atomic orbitals s, p under strong confinement. This result suggests a model, at least of pedagogical interest, to interpret the basic properties of carbon atom in chemistry.

1. INTRODUCTION

Bound states of free atoms or molecules are associated with wave functions that are quadratically integrable when the spatial integration extends over all space. As a consequence, the eigenfunction of the Schrödinger equation tends to zero when one of the particles belonging to the system goes to infinity. When the atoms or the molecules are confined by impenetrable surfaces, the wave function vanishes on these repulsive surfaces. When the atom is inside an impenetrable sphere, this corresponds to an ideal model related to an approximation of the physical reality. The solutions of the Schrödinger equation fulfill the so-called Dirichlet boundary conditions. The model of a spatially confined atom is not just of pedagogic interest. The properties of atoms and molecules undergo drastic changes when they are spatially confined in either penetrable or impenetrable surfaces. This topic has been attracting a lot of attention, and it has become a field of active research. During the last 70 years this model has proved to be quite useful in a number of fields of physics: the effect of pressure on properties, such as the atomic compressibility, the filling of the energy levels, the polarizability or the ionization threshold of atoms and molecules,[1−3] and artificial atoms like quantum dots[4] and in several other areas, like astrophysics and chemistry.[5] Since then many studies investigating various aspects of confined hydrogen atom by employing different approaches have been reported in the literature. We refer the reader to the reviews.[6−8]

The resolution of the Schrödinger equation with Dirichlet boundary conditions is a difficult problem, and to the best of our knowledge, accurate results exist only for low-Z atoms and few-electrons diatomic molecules. The Rayleigh−Ritz variational method is one of the most popular method for calculating accurately the ground- or excited-state energy of an atomic or a molecular system. Its extension to confined systems with more electrons is an important point.

Within the variational approximation, the variational Monte Carlo (VMC) method has been extensively applied to study free complex atoms and molecules obtaining accurate results.[9,10] In the most widely employed implementations, the trial wave function is written as the product of two factors. One factor is completely antisymmetric to account for the fermionic character of the electrons, while the other is symmetric and is tailored to describe the electronic correlations. A third correlation mechanism,[10] based on nonhomogeneous backflow transformations that introduces a dependence of the orbitals in the position of the other electrons, has been employed obtaining very accurate results in atomic, molecular, and extended systems.[11−13]

It is tempting to introduce in the second function a factor to take into account the Dirichlet boundary condition that the wave function vanishes on the impenetrable surfaces. Several forms for such cutoff function to satisfy the Dirichlet boundary condition have been proposed and employed in different works. External potentials, like harmonic oscillator potentials,

Received: April 25, 2011
Published: August 04, 2011

have been used to describe confined quantum system in different symmetries, including oblate symmetries when confined molecules are studied.[14,15]

The purpose of this paper is to extend the VMC method to study confined systems. Taking explicitly into account the Dirichlet boundary condition, we will derive a functional which is quasi identical to the functional used for nonconfined systems. The present work opens the possibility to start from the available function for unbound systems and to analyze the changes of these systems under confinement in a straightforward and flexible manner with little changes in the VMC codes. We illustrate the applicability of this approach by calculating ground- and excited-state energy of confined atoms in different symmetries.

The remaining of the paper is organized in the following manner. In Section 2 the theoretical methods employed in this paper are presented. Section 3 is devoted to the discussion of the results. The paper is concluded in Section 4. Atomic units are used throughout this work.

2. THEORY

2.1. Dirichlet Boundary Conditions and VMC Approach. Let us consider a general Hamiltonian, H, of a quantum system of n interacting particles:

$$H = -\frac{1}{2}\sum_{i=1}^{n}\nabla_i^2 + V(\mathbf{r}_1, ..., \mathbf{r}_n)$$

where the first sum is the kinetic energy operator and V stands for the potential energy operator of the n particles.

The VMC method is based on the variational approach with expectation values calculated by using random walks. The variational approach starts from a judicious choice for the ansatz of a many-body wave function satisfying various properties in accordance with the system under consideration. For unbounded systems, the integration volume in the spatial coordinates is R^{3n}, and the trial wave function vanishes at the infinity. In order to account for confinement by impenetrable surfaces a cutoff factor, w, vanishing at the boundary surface, $\partial\tau$, is included in the variational ansatz:

$$\Psi_t(\mathbf{r}_1, ..., \mathbf{r}_n) = \Psi_f(\mathbf{r}_1, ..., \mathbf{r}_n)w(\mathbf{r}_1, ..., \mathbf{r}_n) \quad (1)$$

where Ψ_f is a trial function for the unbound system.

For brevity, in the following we will use the notation, $\Psi_t(\mathbf{r}_i) = \Psi_t(\mathbf{r}_1, ..., \mathbf{r}_n)$, $\Psi_f(\mathbf{r}_i) = \Psi_f(\mathbf{r}_1, ..., \mathbf{r}_n)$, $w(\mathbf{r}_i) = w(\mathbf{r}_1, ..., \mathbf{r}_n)$ and $\nabla_{3n} = \sum_i \nabla_i$ so that the expressions $\nabla_{3n}^2 w(r_i)$ and $\nabla_{3n} w(r_i)$ stand for the $3n$ dimension laplacian and the gradient, respectively, of the $3n$ variables function $w(r_i)$ or $\Psi_f(\mathbf{r}_i)$. The expectation value of the Hamiltonian with properly normalized trial functions can be written as follows:

$$\langle H\rangle_{\Psi_t} = \int_{\tau(\partial\tau)}\left[-\frac{w(\mathbf{r}_i)^2\Psi_f(\mathbf{r}_i)\nabla_{3n}^2\Psi_f(\mathbf{r}_i)}{2} - \frac{\Psi_f^2(\mathbf{r}_i)w(\mathbf{r}_i)\nabla_{3n}^2 w(\mathbf{r}_i)}{2} - \Psi_f(\mathbf{r}_i)w(\mathbf{r}_i)\nabla_{3n}\Psi_f(\mathbf{r}_i)\cdot\nabla_{3n}w(\mathbf{r}_i) + \Psi_t^2(\mathbf{r}_i)V(\mathbf{r}_i)\right]d\tau \quad (2)$$

where $\tau(\partial\tau)$ represents the volume enclosed by the surface $\partial\tau$. The term with the gradients can be simplified by using

$$\int_{\tau(\partial\tau)}[\Psi_f(\mathbf{r}_i)\nabla_{3n}\Psi_f(\mathbf{r}_i)]\cdot[w(\mathbf{r}_i)\nabla_{3n}w(\mathbf{r}_i)]d\tau = \frac{1}{4}\int_{\tau(\partial\tau)}\nabla_{3n}w^2(\mathbf{r}_i)\cdot\nabla_{3n}\Psi_f^2(\mathbf{r}_i)d\tau$$

and applying a Green transformation:

$$\int_{\tau(\partial\tau)}\nabla_{3n}w^2(\mathbf{r}_i)\cdot\nabla_{3n}\Psi_f^2(\mathbf{r}_i)d\tau = \int_{\partial\tau}\Psi_f^2(\mathbf{r}_i)\nabla_{3n}w^2(\mathbf{r}_i)\cdot d\mathbf{s} - \int_{\tau(\partial\tau)}\Psi_f^2(\mathbf{r}_i)\nabla_{3n}^2w^2(\mathbf{r}_i)d\tau$$

In the latter equation the surface term vanishes because of the Dirichlet condition, $w(r_i) = 0$ when $r_i \in \partial\tau$, and the volume term can be rewritten as follows

$$\int_{\tau(\partial\tau)}\Psi_f^2(\mathbf{r}_i)\nabla_{3n}^2w^2(\mathbf{r}_i)d\tau = 2\int_{\tau(\partial\tau)}\Psi_f^2(\mathbf{r}_i)w(\mathbf{r}_i)\nabla_{3n}^2w(\mathbf{r}_i)d\tau + 2\int_{\tau(\partial\tau)}\Psi_f^2(\mathbf{r}_i)\nabla_{3n}w(\mathbf{r}_i)\cdot\nabla_{3n}w(\mathbf{r}_i)d\tau$$

the first integral cancels out when substituted in the expectation value of the Hamiltonian, eq 2, obtaining

$$\langle H\rangle_{\Psi_t} = \int_{\tau(\partial\tau)}|\Psi_f(\mathbf{r}_i)|^2\left\{w(\mathbf{r}_i)^2E_L^f(\mathbf{r}_i) + \frac{1}{2}[\nabla_{3n}w(\mathbf{r}_i)]^2\right\}d\tau \quad (3)$$

$$= \int_{\tau(\partial\tau)}|\Psi_t(\mathbf{r}_i)|^2\left\{E_L^f(\mathbf{r}_i) + \frac{1}{2}[\nabla_{3n}\ln w(\mathbf{r}_i)]^2\right\}d\tau \quad (4)$$

where

$$E_L^f(\mathbf{r}_i) \equiv \frac{H\Psi_f(\mathbf{r}_i)}{\Psi_f(\mathbf{r}_i)}$$

These expressions provide the energy for a system under constrains defined by the choice of the cutoff function w. The estimator for unbound systems is recovered by making $w(\mathbf{r}_i) \equiv 1$ and extending the surface to infinity

$$\langle H\rangle_{\Psi_f} = \int_{\tau(\infty)}|\Psi_f(\mathbf{r}_i)|^2E_L^f(\mathbf{r}_i)d\tau$$

Extension of these equations to non-normalized trial wave functions is straightforward. Equations 3 and 4 are specially suited for VMC calculations. Calculations for bounded systems can be carried out starting from these equations with minor changes in a VMC code.

2.2. Dirichlet Boundary Conditions and Diffusion Monte Carlo (DMC) Approach. To improve the energies of the atoms, in particular for the carbon atom calculated below, with the wave functions proposed in this work, we have also used them as trial functions in a quantum Monte Carlo calculation. The results are presented below in Section 3.4. More specifically, we shall use in this work the so-called diffusion Monte Carlo (DMC) method. We recall briefly here the main ideas underlying the DMC approach. Further details relative to this powerful approach to solve the

Schrödinger by simulating the Green's function of the system in question by statistical methods can be found in, e.g., refs 9 and 10.

DMC method starts from the time-dependent Schrödinger equation in imaginary time that becomes the classical diffusion equation. To determine the random walk that simulates the diffusion, the Green's function at short time approximation is invoked. Then a step of the random walk consists in an isotropic Gaussian diffusion and branching processes of the walkers. After a large number of iterations, the excited-state contributions are projected out from the initial ensemble, converging to the ground-state wave function, and the ground-state energy can be deduced.

Fermi systems, as those studied in this work, are affected by sing problems resulting from the required antisymmetry of the wave function. Here we will employ the fixed node approximation that uses a prefix nodal surface, including the Dirichlet boundary conditions, in the configuration space of the system. For fermions systems, the fixed node diffusion DMC can be thought of as a super variational approach with an energy which is guaranteed to be closer than the value given by the VMC with the same wave function to the exact one. The results so calculated are not exact anymore, instead an upper bound for the energy is obtained. The accuracy of such bound is governed by the quality of the nodal surface employed in the simulation. This is the most commonly used approach in the literature.

The algorithm, as described above, is in general very inefficient due to the large fluctuations in the ensemble along the random walk introduced by the interaction potential. Practical implementations usually make use of the Monte Carlo technique known as importance sampling that greatly reduces these fluctuations. This method requires an analytical trial function that is used to bias the random walk. However, very involved parametrizations, which generally are time-consuming, will slow down the calculation due to the fact that in each step the gradient and the laplacian must be calculated for each walker. Hence, compact and concise and still accurate wave functions are ideal. The choice of an adequate trial wave function that affects the statistical error in the calculation is very important. For fermion systems, the trial wave function not only affects the statistical error of the calculation but also to the value obtained for the energy. This comes from the fact that the trial wave function also determines the location of the nodal surface. In general, very little is known about the exact location of the nodes in fermion systems. The quality of the nodes structure induced by the trial wave function will determine how close one can come to the exact result. This is usually established a posteriori for those systems for which exact or quasi-exact solutions are available by other methods.

2.3. Determination of the Wave Function and the Energy for Confined Few-Electron Atoms. The atomic Hamiltonian considered here is

$$H = -\frac{1}{2}\sum_{i=1}^{n}\nabla_i^2 - \sum_{i=1}^{n}\frac{Z}{r_i} + \sum_{i<j}\frac{1}{r_{ij}} \tag{5}$$

Bound states are calculated within the variational approximation starting from the trial wave function given in eq 1, i.e., the product of a trial function for the unbound system times a cutoff factor. For the trial function of the unbound system, we use

$$\Psi_f(\mathbf{r}_i) = \Phi_0(\mathbf{r}_i)J(\mathbf{r}_i) \tag{6}$$

The function $\Phi_0(\mathbf{r}_i)$ is the model function and takes into account the antisymmetry of this fermionic system. The $J(\mathbf{r}_i)$ factor describes the correlation between the electrons and is chosen to be positive. This correlation factor usually includes variational parameters and different functional forms are available in the literature to describe accurately the electronic correlation up to relatively large systems.[16,17] In the present work we will use a simple wave function including only three parameters. The main advantage of employing a simple few-parameters wave function is to provide an easy physical insight on the behavior of interelectronic correlation with the variation in the confinement parameter.

In all of the different applications of this work, the model function $\Phi_0(\mathbf{r}_i)$ is chosen such that it satisfies the Schrödinger equation for n noninteracting electrons moving in a nuclear potential with electric charge Z:

$$\left[\sum_{i=1}^{n}\left(-\frac{1}{2}\nabla_i^2 - \frac{Z}{r_i}\right)\right]\Phi_0(r_i) = E_0\Phi_0(\mathbf{r}_i) \tag{7}$$

Then the expression for the energy, eq 4 reduces to

$$\langle H\rangle_{\Psi_t} = E_0 + \int_{\tau(\partial\tau)}|\Psi_t(\mathbf{r}_i)|^2\left\{\frac{1}{2}[\nabla_{3n}\ln(J(\mathbf{r}_i)w(\mathbf{r}_i))]^2 + \sum_{i<j}\frac{1}{r_{ij}}\right\}d\tau \tag{8}$$

The total energy of a n-electron atomic system is decomposed into two parts: E_0 representing the energy of the free n noninteracting electrons moving in an attractive potential of nucleus with charge Z and a second term accounting for the electron−electron repulsion energy, electronic correlations, and cutoff conditions. This expression is convenient for carrying out variational calculations. In the following we apply it to study confined helium, lithium, and carbon atoms with different boundary conditions.

2.4. Explicit Wave Function for Few-Electron Systems. *2.4.1. Helium Atom.* Three different confinements, spherical, two planes, and cylindrical, have been considered for the helium atom. This is done by using different forms of the confinement function $w(\mathbf{r}_i)$. Different expressions for the cutoff function, linear, quadratic, step-like function, have been considered in the literature.[18] The functional form for the cutoff function $w(r_i)$ used in this work was proposed by Laughlin and Chu.[19] It is extended here to the different geometries considered. In a recent work[20] the accuracy of this choice for the cutoff on the confined ground state of hydrogen atom has been studied. The exact solution of the latter atom is known under Dirichlet boundary conditions, and this allows a check of the accuracy of the different forms of the cutoff functions. Additional calculations made on the confined helium atom in spherical surfaces show also the validity of this choice for the cutoff function.

For an atom located at the center of an impenetrable sphere of radius r_c, the cutoff function is taken as

$$w_{\text{spherical}}(r_i) = \prod_{i=1}^{n}\left(1 - \frac{r_i}{r_c}\right)\exp\left(\frac{r_i}{r_c}\right) \tag{9}$$

When the atom is located on the z axis of a impenetrable cylinder, axial symmetry, of radius ρ_c, $w_{\text{cylindical}}$ is

$$w_{\text{cylindrical}}(\rho_i) = \prod_{i=1}^{n}\left(1-\frac{\rho_i}{\rho_c}\right)\exp\left(\frac{\rho_i}{\rho_c}\right) \tag{10}$$

where $\rho_i^2 = x_i^2 + y_i^2$. Finally, to describe an helium atom confined between two parallel impenetrable planes located at $\pm z_c$ the following cutoff function is employed

$$w_{\text{planar}}(z_i) = \prod_{i=1}^{n}\left(1-\frac{|z_i|}{z_c}\right)\exp\left(\frac{|z_i|}{z_c}\right) \tag{11}$$

We study both, the ground state and the first ^{3}S excited state. For both states Φ_0 is written as a Slater determinant

$$\Phi_0^{1S} = \frac{1}{\sqrt{2!}}\det\{\varphi_{100}|\uparrow\rangle, \varphi_{100}|\downarrow\rangle\}$$

$$\Phi_0^{3S} = \frac{1}{\sqrt{2!}}\det\{\varphi_{100}|\uparrow\rangle, \varphi_{200}|\uparrow\rangle\}$$

with $|\uparrow\rangle$ and $|\downarrow\rangle$ the electronic spin part and

$$\varphi_{nlm}(\mathbf{r}) = R_{nl}(r)Y_{lm}(\Omega)$$

with $Y_{lm}(\Omega)$ the spherical harmonic and R_{nl}

$$R_{10}(r) = 2Z^{3/2}e^{-Zr}, \quad R_{20}(r) = \frac{Z^{3/2}}{\sqrt{2}}\left(1-\frac{Z}{2}r\right)e^{-Z/2r}$$

has already been proposed in a previous paper .[21]

For the correlation factor, we use the following form

$$J(\mathbf{r}_1,\mathbf{r}_2) = [\cosh(\lambda r_1) + \cosh(\lambda r_2)]\exp\left(\frac{br_{12}}{1+ar_{12}}\right) \tag{12}$$

so that the trial function, eq 1, for these two states of the confined helium atom is

$$\Psi_t(\mathbf{r}_i) = [\Phi_0^{1S} \text{ or } \Phi_0^{3S}]J(\mathbf{r}_i)w(\mathbf{r}_i)$$

with w any of the three cutoff factors given in eqs 9, 10, or 11. This function satisfies the electron−electron cusps conditions governing the interaction for the short interelectronic distances and the electron−nucleus cusps conditions. The parameter λ is interpreted as a screening constant for one electron when it is located far away from the nucleus. The relevant part of the wave function representing the latter property is

$$\cosh(\lambda r_i)\exp(-Zr_i) \approx \exp[-(Z-\lambda)r_i]r_i \gg 1 \tag{13}$$

Such function, though very simple, is accurate and convenient for the calculation.

The expectation value of the energy has been calculated by using eq 8. The integral has been evaluated by using the VMC method with Metropolis sampling. Analytical expressions for $|\nabla(Jw)|^2$ can be obtained in a straightforward manner.

2.4.2. Lithium Atom. The wave function for the lithium atom ground, $1s^22s\ ^2S$ and $1s^22p\ ^2P$, and, $1s^23d\ ^2D$, excited states is a direct extension to the three-electron system of the previous one. For this atom we will consider spherical confinement only.

The Slater determinant part is built starting from hydrogenic orbitals ϕ_{nlm}

$$\Phi_0^{2S} = \frac{1}{\sqrt{3!}}\det\{\varphi_{100}|\uparrow\rangle, \varphi_{100}|\downarrow\rangle, \varphi_{200}|\uparrow\rangle\}$$

$$\Phi_0^{2P} = \frac{1}{\sqrt{3!}}\det\{\varphi_{100}|\uparrow\rangle, \varphi_{100}|\downarrow\rangle, \varphi_{210}|\uparrow\rangle\}$$

$$\Phi_0^{2D} = \frac{1}{\sqrt{3!}}\det\{\varphi_{100}|\uparrow\rangle, \varphi_{100}|\downarrow\rangle, \varphi_{320}|\uparrow\rangle\}$$

The spherical confinement, eq 9, is used for the cutoff function w. For the correlation factor, a product of two terms, one depending on the interelectronic distance and the other on the electron−nucleus distance, is employed

$$J(\mathbf{r}_i)w(\mathbf{r}_i) = \left\{\sum_{i<j}^{3}[\cosh(\lambda r_i)\cosh(\lambda r_j)]\prod_{i<j}^{3}\exp\left(\frac{br_{ij}}{1+ar_{ij}}\right)\right\}\left\{\prod_{i=1}^{3}\left(1-\frac{r_i}{r_c}\right)e^{r_i/r_c}\right\} \tag{14}$$

The trial wave functions for these three states Φ_0^{2S}, Φ_0^{2P}, and Φ_0^{2D} of the lithium atom under spherical confinement read

$$\Psi_t(\mathbf{r}_i) = [\Phi_0^{2S} \text{ or } \Phi_0^{2P} \text{ or } \Phi_0^{2D}]J(\mathbf{r}_i)w(\mathbf{r}_i) \tag{15}$$

Note that the factor depending on the interelectronic distance is of the same form as that employed for the helium atom. For the other factor, a pair product form employed in a previous work[22] is used because it provides a better performance from the variational point of view.

2.4.3. Carbon Atom. We focus on the carbon atom in order to study the effect of the spherical confinement on the electronic configuration. In particular we aim to compare the behavior under confinement of the ground state ^{3}P wave function of carbon atom with that of the hybridized configuration sp^3. The hybridized atomic orbitals are employed in quantum chemistry calculations to account for the valence of this atom. In doing so, two different orbital sets to build Φ_0 are considered.

In order to describe the ^{3}P ground state a single Slater determinant can be used

$$\Phi_0^{3P} = \frac{1}{\sqrt{6!}}\det\{\varphi_{100}|\uparrow\rangle, \varphi_{100}|\downarrow\rangle, \varphi_{200}|\uparrow\rangle, \varphi_{200}|\downarrow\rangle, \varphi_{211}|\uparrow\rangle, \varphi_{210}|\uparrow\rangle\} \tag{16}$$

with the form of the orbitals given above and

$$R_{21}(r) = \frac{Z^{3/2}}{2\sqrt{6}}Zre^{-Z/2r}$$

Hybrid orbitals are symmetry adapted atomic orbitals because they are constructed to provide a basis of atomic orbitals consistent with the observed structure of the molecules, e.g., ref 23. This is done by taking linear combinations to form a basis for a representation of the point symmetry group of the

Table 1. Ground-State Energy and Radial Expectation Values for the Helium Atom under Different Constraints for Some Values of the Constraint Distance [a]

d_c	const	λ	E	E_{Hyll}	$\langle r\rangle$	$\langle r_{ij}\rangle$
1.0	3D	0.00	1.01866(4)	1.015755	0.44279(2)	0.64795(4)
	2D	0.05	−0.52859(7)		0.55925(5)	0.83369(9)
	1D	0.50	−1.86606(6)		0.71691(8)	1.0825(1)
1.1	3D	0.50	0.01077(3)		0.47795(2)	0.70122(4)
	2D	0.45	−1.14577(7)		0.59531(5)	0.8891(1)
	1D	0.60	−2.14097(6)		0.74635(9)	1.1284(2)
1.2	3D	0.70	−0.70744(2)		0.51274(2)	0.75411(5)
	2D	0.575	−1.58350(7)		0.62662(5)	0.9373(3)
	1D	0.65	−2.33433(7)		0.76839(9)	1.1627(2)
1.3	3D	0.825	−1.22999(2)		0.54636(3)	0.80542(5)
	2D	0.675	−1.90036(6)		0.65777(6)	0.9855(1)
	1D	0.70	−2.47314(6)		0.79125(9)	1.1986(2)
1.4	3D	0.90	−1.61647(2)		0.57798(3)	0.85338(5)
	2D	0.75	−2.13348(6)		0.68731(6)	1.0315(1)
	1D	0.725	−2.57454(6)		0.80819(9)	1.2250(2)
1.5	3D	0.95	−1.90621(2)		0.60783(3)	0.89991(6)
	2D	0.80	−2.30743(6)		0.71376(7)	1.0727(1)
	1D	0.75	−2.64948(5)		0.82477(9)	1.2511(2)
2.0	3D	1.05	−2.60303(2)	−2.604038	0.73327(4)	1.09582(7)
	2D	0.90	−2.72192(4)		0.81224(7)	1.2275(1)
	1D	0.80	−2.82508(4)		0.87972(9)	1.3379(2)
3.0	3D	1.0	−2.87060(2)	−2.872495	0.87392(7)	1.3228(1)
	2D	0.875	−2.88044(3)		0.89839(8)	1.3660(1)
	1D	0.80	−2.89118(3)		0.9231(1)	1.4075(2)
4.0	3D	0.9	−2.89883(2)	−2.900485	0.91761(9)	1.3964(2)
	2D	0.825	−2.89856(2)		0.9237(1)	1.4078(2)
	1D	0.775	−2.89954(2)		0.9325(1)	1.4229(2)
5.0	3D	0.85	−2.90188(2)	−2.903410	0.93475(9)	1.4258(2)
	2D	0.80	−2.90127(2)		0.9347(1)	1.4262(2)
	1D	0.75	−2.90114(2)		0.9314(1)	1.4211(2)
6.0	3D	0.85	−2.90121(2)	−2.903696	0.9538(1)	1.4578(2)
	2D	0.775	−2.90179(2)		0.9353(1)	1.4274(2)
	1D	0.75	−2.90152(2)		0.9361(1)	1.4289(2)
10.0	3D	0.75	−2.90196(2)	−2.903724	0.9355(1)	1.4279(2)
	2D	0.725	−2.90185(2)		0.9291(1)	1.4173(2)
	1D	0.725	− 2.90177(2)		0.9325(1)	1.4229(2)
20.0	3D	0.75	− 2.90179(2)	−2.903724	0.9333(1)	1.4242(2)
	2D	0.725	−2.90178(2)		0.9340(1)	1.4255(2)
	1D	0.725	−2.90178(2)		0.9348(1)	1.4267(2)

[a] 3D stands for spherical, 2D for cylindrical, and 1D for two plane impenetrable surfaces. The energy in the 3D case is compared with the highly accurate value, E_{Hyll}, of Laughlin and Chu[19] calculated by using Hylleraas-type basis functions. In parentheses we show the statistical error in the last digit.

molecule. For example, the four sp^3 hybrid orbitals of the carbon atom form a basis for a representation of the group T_d and are given as

$$\varphi_1 = \frac{1}{2}(2s + 2p_x + 2p_y + 2p_z),$$
$$\varphi_2 = \frac{1}{2}(2s + 2p_x - 2p_y - 2p_z) \quad (17)$$
$$\varphi_3 = \frac{1}{2}(2s - 2p_x + 2p_y - 2p_z),$$
$$\varphi_4 = \frac{1}{2}(2s - 2p_x - 2p_y + 2p_z) \quad (18)$$

where p_x, p_y, and p_z are the real spherical harmonics. The spatial distribution of the sp^3 orbitals is such that the directions of maximum density point from the center of the tetrahedron to its corners. Therefore, these atomic hybrid orbitals of the carbon atom are specially suited to build molecular orbitals of compounds like methane.

Starting from the hybrid sp^3 orbitals given in eq 18 a Slater determinant $\Phi_0^{sp^3}$ is built

$$\Phi_0^{sp^3} = \frac{1}{\sqrt{6!}}\det\{\varphi_{100}|\uparrow\rangle, \varphi_{100}|\downarrow\rangle, \varphi_1|\uparrow\rangle, \varphi_2|\downarrow\rangle, \varphi_3|\uparrow\rangle, \varphi_4|\uparrow\rangle\} \quad (19)$$

To study the performance of both set of orbitals for confined carbon atom, the spherical confinement is considered. For the correlation and confinement factors, the following form is employed

$$J(\mathbf{r}_i)w(\mathbf{r}_i) = \left\{\prod_{i=1}^{6}\cosh(\lambda r_i)\prod_{i<j}^{6}\exp\left(\frac{br_{ij}}{1+ar_{ij}}\right)\right\}\left\{\prod_{i=1}^{6}\left(1-\frac{r_i}{r_c}\right)e^{r_i/r_c}\right\} \quad (20)$$

The two trial wave functions employed for the ground state of the carbon atom under spherical confinement are

$$\Psi_t = [\Phi_0^{3p} \text{ or } \Phi_0^{sp^3}]J(\mathbf{r}_i)w(\mathbf{r}_i) \quad (21)$$

3. RESULTS AND DISCUSSION

This section presents the results obtained with the correlated wave function proposed in the previous section. They are compared with the data in the literature when available. The present trial wave function has only three variational parameters. They have been first optimized for the free systems. When the constraint is added we have also optimized these parameters. We found that among the three parameters a, b, and λ, the optimized values of the parameters a and b do not vary significantly along the confinement radius r_c in all the atoms studied here. For this reason we present in the tables the results obtained with fixed values for a and b = 0.5 determined at once for the free system. The λ parameter is optimized for the different values of the constraint distances r_c, ρ_c, or z_c.

This suggests that for the atoms studied here the interelectronic correlation remains almost unaffected by the confining potential, and the major contribution of this part of the energy comes from close interelectronic distances, cusps conditions, that are favored by the strong confining conditions. For the atoms studied here this is in agreement with the observation made by Ludeña who noted that the correlation energy is largely independent of the size of the enclosing sphere .[24] This conclusion cannot be straightforwardly extended to confined heavier atoms where[2] first relativistic effects are important, and second the use

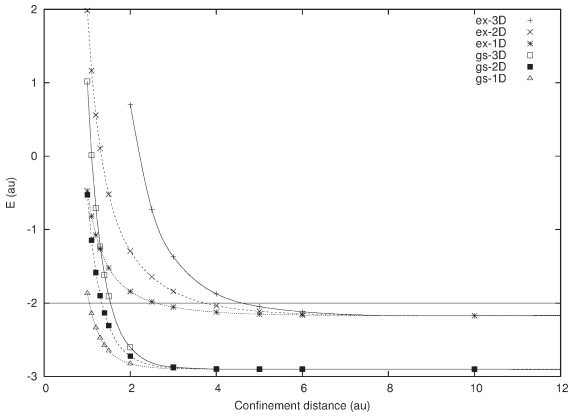

Figure 1. Total energy at different confinement distances for the He atom ground state, *gs* values, and 2^3S excited state, *ex* values. The 3D stands for spherical, 2D for cylindrical, and 1D for two plane impenetrable surfaces. The lines are for guiding the eyes. Statistical error is smaller than the symbol size.

of the Dirichlet boundary condition to model confinement is not relativistically consistent.

3.1. Confined Helium Ground State. The energy values for helium ground state under different constrains: spherical (3D), axial (2D), and planar (1D) are reported in Table 1. The corresponding values are plotted in Figure 1. In all of the cases, it can be remarked that the energies are increased when the constraint is stronger. The raise in energy is more important when the atom is located at the center of a impenetrable sphere than on the axis of a impenetrable cylinder or in the middle between two impenetrable planes. The assumption that the atom lies at the center of a repulsive sphere is an exact result in this case, but it should not be extended when the surface is attractive, like a fullerene surface. The values for ground state in the 3D constraint are in good agreement with the highly accurate energies obtained from expansions in terms of Hylleraas-type basis functions, results included in Table 1, and also with other data available in the literature, see ref 19 and references therein. In this respect it is very useful to evaluate and test a new approach. To the best of our knowledge, no other data are presently available for 2D or 1D constrains. It might be of interest to note that in the latter constrains (2D, 1D), the space allowed to the atom is still infinite and, however, a significant effect of the confinement results. Such constraint is similar to the constraint for excitons in quantum wire (2D) or quantum well (1D). In Table 1 the radial expectation values $\langle r\rangle$ and $\langle r_{ij}\rangle$ calculated in the different constraints are also reported. It can be seen that for the ground state, both $\langle r\rangle$ or $\langle r_{ij}\rangle$ decrease with the constraint distance for all kind of confinements. The effect of confinement on these quantities is larger for the 3D than the 2D and 1D constraints.

3.2. Confined Helium Excited State ^{3}S. For excited states the wave function is more diffuse in the space, and the raise in energy is expected to be significant at larger values of the constraint than in the case of the ground state. In Table 2 we report the values of the energies for the helium He(1s,2s) ^{3}S excited state. These results are plotted in Figure 1. The raise in energy is significant at $r_c = 6$ au for 3D constraint and around ρ_c, $z_c = 4$ au for cylindrical and planar constrains, respectively. The ionization of the excited helium atom occurs when the energy of this atom is equal to the energy of the compressed ion $He(1s)^+$, which is practically equal to $E = -2$ au in this range of r_c, ρ_c, z_c values. With the help of the results shown in Figure 1 it can be obtained that this energy value is reached for $r_c \approx 4.5$ au, $\rho_c \approx 4$ au and $z_c \approx 3$ au.

In Figure 2 the expectation value $\langle r_{ij}\rangle$ determined for the different constraints are plotted. For the closed 3D constraint the $\langle r_{ij}\rangle$ values decrease obviously at all the values of r_c. But for 2D and 1D constraint, the space is still infinite, and $\langle r_{ij}\rangle$ decreases down to $\rho_c = 4$ au and $z_c = 3$ au and increases again. These values should be related to the corresponding values of these parameters for the ionization as determined above. The situation is significantly different for the ground state.

Table 2. Total Energy and Radial Expectation Values of the 2^3S Excited State of the Helium Atom under Different Constraints for Some Values of the Constraint Distance[a]

d_c	const	λ	E	$\langle r\rangle$	$\langle r_{ij}\rangle$
1.0	3D				
	2D	0.675	1.9839(4)	2.915(2)	5.343(4)
	1D	0.475	−0.4736(2)	2.3696(6)	4.179(1)
1.1	3D				
	2D	0.7	1.1636(4)	3.159(2)	5.808(4)
	1D	0.475	−0.8189(2)	2.3754(6)	4.182(1)
1.2	3D				
	2D	0.7	0.5604(3)	3.167(2)	5.810(4)
	1D	0.475	−1.0717(1)	2.3819(6)	4.187(1)
1.3	3D				
	2D	0.7	0.1053(3)	3.173(2)	5.806(4)
	1D	0.5	−1.2610(1)	2.4925(6)	4.396(1)
1.5	3D				
	2D	0.7	−0.5205(2)	3.179(2)	5.796(4)
	1D	0.5	−1.52170(9)	2.5035(6)	4.407(1)
2.0	3D	0	0.7004(2)	0.93115(3)	1.46115(6)
	2D	0.6	−1.2916(1)	2.4285(9)	4.279(2)
	1D	0.475	−1.84207(6)	2.4180(5)	4.221(1)
2.5	3D	0	−0.72776(7)	1.0919(4)	1.73303(8)
	2D	0.55	−1.64206(8)	2.2050(6)	3.822(1)
	1D	0.45	−1.98126(3)	2.3449(4)	4.0692(8)
3.0	3D	0	−1.36873(2)	1.22921(5)	1.97062(8)
	2D	0.5	−1.83986(5)	2.0632(5)	3.5342(9)
	1D	0.45	−2.05443(2)	2.3657(4)	4.1031(8)
4.0	3D	0.4	−1.87388(1)	1.51565(6)	2.4750(1)
	2D	0.45	−2.03480(2)	2.0360(3)	3.4668(6)
	1D	0.45	−2.12324(1)	2.4141(4)	4.1899(8)
5.0	3D	0.475	−2.04758(1)	1.75936(8)	2.9210(1)
	2D	0.45	−2.11193(1)	2.1447(3)	3.6683(6)
	1D	0.45	−2.15081(1)	2.4645(4)	4.2844(7)
6.0	3D	0.5	−2.11740(1)	1.9631(1)	3.3035(2)
	2D	0.475	−2.14463(1)	2.3067(3)	3.9769(5)
	1D	0.45	−2.16287(1)	2.5124(4)	4.3761(8)
10.0	3D	0.5	−2.17191(1)	2.4563(2)	4.2545(4)
	2D	0.45	−2.17235(1)	2.5157(3)	4.3804(6)
	1D	0.425	−2.17290(1)	2.6387(4)	4.6204(7)
20.0	3D	0.45	−2.17442(1)	2.6045(4)	4.5457(8)
	2D	0.425	−2.17410(1)	2.5927(4)	4.5309(8)
	1D	0.425	−2.17400(1)	2.6159(4)	4.5762(7)

[a] 3D stands for spherical, 2D for cylindrical, and 1D for two plane impenetrable surfaces. In parentheses we show the statistical error in the last digit.

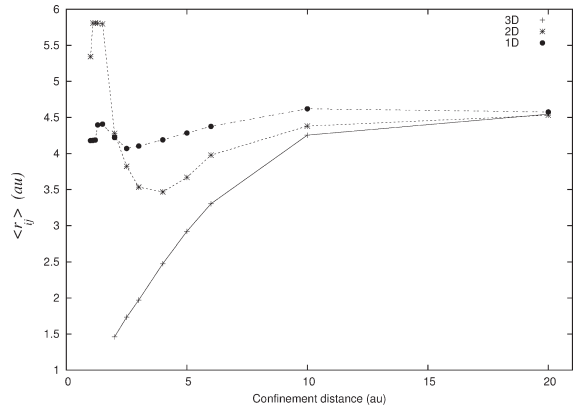

Figure 2. Expectation value of the interelectronic distance as a function of the confinement parameter for the 2^3S excited state of the He atom. The 3D stands for spherical, 2D for cylindrical, and 1D for two planes impenetrable surfaces. The lines are for guiding the eyes. Statistical error is smaller than the symbol size.

3.3. Confined Lithium Atom. The results for this three-electron system, ground state ^2S and excited states ^2P and ^2D, confined in an impenetrable sphere are determined by using fully correlated wave function given by eq 15 are presented in Table 3 and also displayed in Figure 3. The results have been obtained with $a = 0.7$, which has been fixed by performing a calculation for a very large value of r_c. Like two-electron systems we do not observe any significant change in the optimized value of the parameter a when r_c is varied, and consequently we use the same value of parameter a ($a = 0.7$) for all the calculations. Only few calculations are available in the literature for the ground state and to the best of our knowledge none exist for excited states. The ground-state energies of ref 24 obtained by using the Hartree–Fock approach are reported in Table 3. We note from Table 3 and Figure 3 that our results for the energy are significantly lower than the Hartree–Fock ones for $r_c > 2$ au. In order to check the accuracy of the correlated wave function, the energy of a confined Li atom with $r_c = \infty$ (uncompressed atom) has been calculated. The ground-state energy obtained with the simple wave function of eq 15 $E = -7.47360(3)$ au is in very a good agreement with the high-precision variational results of Yan and Drake[25] $E = -7.478060$ au calculated by using multiple basis sets in Hylleraas coordinates. As stated above, the optimized value of the parameter a remains constant at all confinement radii. This suggests that the electron–electron interaction is almost independent of the confinement. This finding is in agreement with a conclusion already drawn by Gimarc[26] who noted that in the case of helium the correlation energy is largely independent of the size of the enclosing sphere.

The λ values are strongly dependent on the confinement as illustrated by the changes in the values of λ in Table 3. Like the confined H^- ion and the He atom, the value of the parameter λ also tends to zero for a strongly confined Li atom. Thus the electronic screening of the nuclear charge by the electrons decreases when the confinement radius becomes small.

The results for the confined lithium atom in the excited state ^2P are reported in Table 3 and plotted in the Figure 3. The energy of the free atom in this state obtained by the present method is $E = -7.40315(4)$ au to be compared to the accurate value[25] $E = -7.410157$ au. When the confinement is stronger, the energy increases. A crossing with the ground state occurs at $r_c = 3.3$ au.

Table 3. Total Energy and Radial Expectation Values of the Ground State $(1s^22s)\ ^2S$ and $(1s^22p)\ ^2P$ and $(1s^23d)\ ^2D$ Excited State in Spherical Confinement as a Function of the Radius[a]

r_c	λ	$\langle r \rangle$	$\langle r_{ij} \rangle$	E	E_{SCF}
			$(1s^22s)\ ^2S$		
1.5	0	0.61113(2)	0.93871(3)	−1.9805(3)	−2.2281
2.0	0.3	0.72939(3)	1.13934(4)	−5.1305(2)	−5.1782
3.0	0.675	0.94861(4)	1.52472(7)	−6.83046(6)	−6.8027
4.0	0.775	1.12640(6)	1.8524(1)	−7.24481(4)	−7.2046
5.0	0.8	1.26424(8)	2.1143(2)	−7.38155(4)	−7.3395
6.0	0.825	1.3853(1)	2.3469(2)	−7.43428(3)	−7.3925
8.0	0.825	1.5370(2)	2.6430(3)	−7.46581(3)	−7.4249
10.0	0.825	1.6289(2)	2.8215(4)	−7.47176(3)	
∞	0.775	1.6855(3)	2.9380(5)	−7.47360(3)	−7.4327
∞	Hyll	1.66317	2.88947	−7.478060	
			$(1s^22p)\ ^2P$		
1.5	0.48	0.60585(2)	0.93232(4)	−3.9142(2)	
2.0	0.7	0.73002(3)	1.13783(4)	−5.7740(1)	
3.0	0.83	0.93032(4)	1.48703(7)	−6.85948(6)	
4.0	0.88	1.09853(7)	1.7956(1)	−7.16837(3)	
5.0	0.92	1.2542(1)	2.0890(2)	−7.28902(3)	
6.0	0.94	1.3888(1)	2.3471(2)	−7.34415(4)	
8.0	0.96	1.6028(2)	2.7628(3)	−7.38536(3)	
10.0	0.96	1.7366(2)	3.0256(5)	−7.39724(4)	
∞	0.95	1.9918(5)	3.5303(9)	−7.40315(4)	
∞	Hyll	1.95712	3.47070	−7.410157	
			$(1s^23d)\ ^2D$		
2.0	0	0.77719(3)	1.21442(5)	−3.6126(3)	
3.0	0	0.97962(4)	1.58763(7)	−5.9095(1)	
4.0	0.35	1.18591(6)	1.9778(1)	−6.61559(9)	
5.0	0.46	1.39216(7)	2.3754(1)	−6.92147(6)	
6.0	0.52	1.5925(1)	2.7664(2)	−7.07723(6)	
8.0	0.60	1.9887(2)	3.5457(4)	−7.21916(5)	
10.0	0.63	2.3322(3)	4.2261(5)	−7.27530(4)	
∞	0.65	3.825(2)	7.201(3)	−7.32579(4)	
∞	Hyll	3.87641	7.28852	−7.335524	

[a] The ground-state results are compared with the self consistent field energy, E_{SCF} of Ludeña,[24] and the results for the unconfined state ($r_c = \infty$) are compared with the very precision values of Yan and Drake,[25] Hyll, calculated by using multiple basis set in Hylleraas coordinates.

Changes of the order of the atomic levels and the ordering of filling of the shells are observed in compressed atoms as already found by different authors, see refs 1 and 3 and references therein.

The results for the confined lithium atom in the excited state ^2D are reported in Table 3 and plotted in the Figure 3. The energy of the free atom in this state obtained form the variational wave function of this work is $E = -7.32579(4)$ au to be compared to the accurate value[25] $E = -7.335524$ au. It is interesting to remark that the rise in energy versus r_c is important and becomes significant at relatively large values of $r_c \simeq 8$ au.

3.4. Confined Carbon Atom. It is well-known that the carbon atom needs a rearrangement of its electronic ground-state configuration $2s^22p^2$ in order to account for molecules such as CH_4. In basic text books an ad hoc hypothesis is made that consists to mix the 2s and 2p orbitals to form four new hybridized

orbitals sp^3, where the four electrons can be placed to form the right number of chemical bounds. This hypothesis is often said to be a purely mathematical device, but necessary, to describe the basic chemical properties of the carbon atom.

We propose here an analysis that might be of pedagogical interest and gives some more physical insight of mechanism of this electronic rearrangement. In this section we show that the mixing of the 2s and 2p orbitals to form the four sp^3 orbitals could be interpreted as a natural consequence of the constraints induced by the surrounding of the carbon, i.e., the protons of hydrogen atoms close to this atom.

The present approach, not dependent on the self consistent field approach, is convenient to calculate the consequence of the confinement by impenetrable sphere on the ground state C $(1s^2 2s^2 2p^2)$ ^3P or hybridized C $(1s^2(2sp^3)^4)$ on the same footing. The values of the energies of the carbon atom in the ^3P and hybridized state sp^3 using the VMC approach are reported at different values of the confinement radii r_c in Table 4. For the free system (no constraint) the ground-state energy of the ^3P calculated with the present simple wave function of eq 21 is $E(^3P) = -37.6786(2)$ au to be compared to the self consistent field energy $E = -37.6886$ au, and the estimated exact energy[27] is $E = -37.8450$ au. The energy of the hybridized configuration sp^3 calculated by the present approach is $E(sp^3) = -37.4793(2)$ au, i.e., 0.199 au above the ground-state energy. When confinement, measured by the cutoff radius r_c, becomes stronger, the energies are raised.

In order to improve the energy of the carbon atom obtained through the VMC approach, we made further calculations using the DMC approach both for the ground state $(1s^2 2s^2 2p^2)$ ^3P and the hybridized C $(1s^2(2sp^3)^4)$ under confinement. The results are displayed in Table 4. It can be noticed that within this approach, the energies are significantly improved respectively $E(^3P) = -37.7996(9)$ au and $E(sp^3) = -37.6333(5)$ au for the free systems, i.e., 0.166 au above the ground-state energy.

In Figure 4 the energy difference $\Delta E = E(^3P) - E(^3sp^3)$, i.e., the threshold of the transition from the ground state to the hybridized one deduced with the VMC and the DMC methods, is plotted versus r_c. A crossing $(\Delta E = 0)$ is found in the neighborhood of $r_c = 1.6$ au. It can be said that the differences between both approaches are small, and the VMC method is able to describe correctly the behavior of the carbon atom under

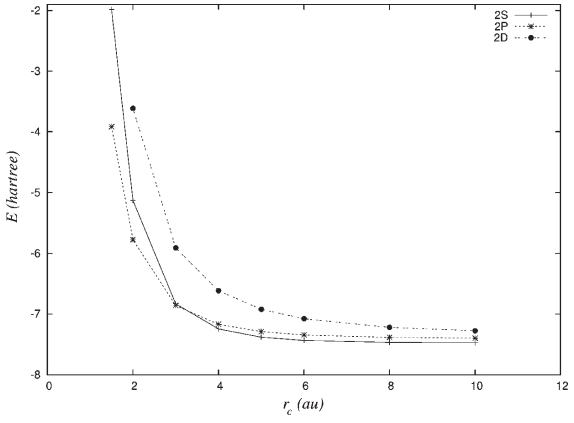

Figure 3. Ground- and excited-state energies of the lithium atom under spherical as a function of the confinement radius, r_c. The lines are for guiding the eyes. Statistical error is smaller than the symbol size.

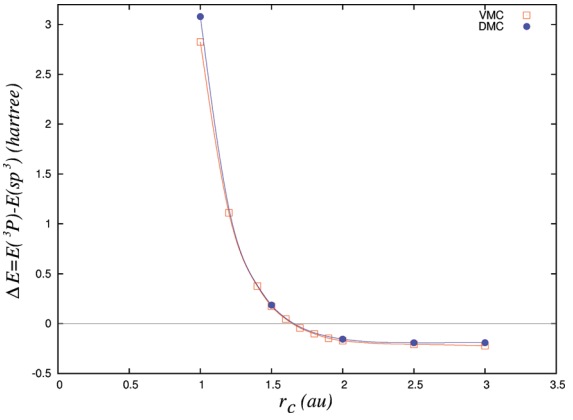

Figure 4. Difference of energy obtained from wave functions built from atomic and orbitals hybrid orbitals for the ground state of the carbon atom surrounded by a nonpenetrable spherical surface of radius r_c. The lines are for guiding the eyes. Statistical error is smaller than the symbol size.

Table 4. Ground-State Energy of the Carbon Atom in Spherical Confinement As a Function of the Radius[a]

r_c	$E_{SCF}(^3P)$	$E_{VMC}(^3P)$	$E_{DMC}(^3P)$	$E_{VMC}(sp^3)$	$E_{DMC}(sp^3)$	$\lambda(^3P)$	$\lambda(sp^3)$
1.0	−10.9178	−10.9832(4)	−11.1042(5)	−13.8081(5)	−14.183(1)	0.008	0.026
1.2		−22.3683(3)		−23.4792(3)		0.040	0.070
1.4		−28.3927(2)		−28.7694(2)		0.25	0.41
1.5	−30.2169	−30.3303(2)	−30.3856(6)	−30.5048(5)	−30.572(3)	0.43	0.52
1.6		−31.8184(2)		−31.8647(2)		0.57	0.62
1.7		−32.9704(2)		−32.9269(2)		0.63	0.69
1.8		−33.8709(4)		−33.7692(2)		0.70	0.74
1.9		−34.5829(8)		−34.4364(2)		0.74	0.79
2.0	−35.0588	−35.1435(2)	−35.2084(6)	−34.9722(2)	−35.0526(9)	0.79	0.83
2.5	−36.6548	−36.6681(3)	−36.7939(6)	−36.4604(3)	−36.6023(8)	0.89	0.93
3.0	−37.2570	−37.2441(3)	−37.3906(7)	−37.0227(3)	−37.200(1)	0.92	0.96
∞	−37.6885	−37.6786(2)	−37.7996(9)	−37.4793(2)	−37.6333(5)	0.84	0.88

[a] In column ^3P column we report the results obtained from Coulomb orbitals, while in sp^3 column we show the energy obtained from hybridized orbitals. In parentheses we show the statistical error in the last figure. The λ parameter in the correlation factor in each calculation is reported. The results are compared with the self consistent field energy, E_{SCF}, of Ludeña.[24]

confinement. The present model, based on a simple impenetrable sphere confinement, shows that the carbon hybridization sp^3 might be understood as due to the confinement by the surrounding atoms when it becomes sufficiently strong. Briefly stated, the spherical confinement has induced a raise in the energy, corresponding to the symmetry group of the ^3P state, equal to the energy of carbon atom in the symmetry group T_d at r_c around 1.6 au.

As explained previously the choice of pure hydrogenic orbitals in the present wave function allows a direct calculation of the nonspectroscopic state. However for the carbon atom the energy calculated within the VMC is a little bit degraded. For the ground state of the unconfined atom, the VMC obtained by using self consistent field orbitals and a more complex correlation factor[11] is $E = -37.8064(3)$, and the fixed node DMC value is $E = -37.8297(2)$.

It is of interest to recall here that the first spectroscopic excited state $2s2p^3\ ^5S^o$ with four unpaired electrons in the carbon atom is about 0.1537 au above the ground state,[28] and it could be a candidate to account for the electronic rearrangement in the carbon atom. However the spin value, $S = 2$, of this term precludes the transition from the, $S = 1$, ground state. The nearest triplet states with four unpaired electrons are[28] the, $2s2p^3\ ^3D^o$ and $2s2p^3\ ^3P^o$, terms with excitation energies of $E = 0.2920$ and 0.3429 au, respectively. Thus as a consequence of this energy gap they cannot easily be populated from the ground state.

The present model suggests that the constraint by the surrounding atoms induces first a transitory state in the carbon atom, the hybridized state, followed by the chemical binding resulting in a stable four bond molecule.

4. CONCLUSIONS

In the present work a functional of the energy has been derived in the framework of the VMC method to study confined systems by nonpenetrable surfaces of different symmetries. The functional has been applied to study ground and excited states of some atoms under different constraints. In all cases the energies of the systems, He, Li, and C, are raised when the confinement parameter becomes stronger. Average values of the interparticle distances (electron−nucleus $\langle r \rangle$ and electron−electron $\langle r_{ij} \rangle$) are also determined.

It is observed that for the first excited ^3S of helium atom, the values of $\langle r_{ij} \rangle$ versus the constraint parameter present a minimum when the confinement results from impenetrable cylinder or planes at values corresponding to the ionization threshold of this excited atom.

The study of the confined carbon atom suggests a possible mechanism responsible of the hybridization of the s,p orbitals of this atom in order to explain the four chemical bonds generally observed with the carbon atom.

We hope that the present extension of the VMC to confined nonrelativistic systems will be useful to study larger systems including molecules. In particular the confinement might play an important role in the chemical reactivity of molecules, even in biology, for example, in enzymatic reactions when the substrate is enclosed in the active site of the enzyme.

AUTHOR INFORMATION

Corresponding Author

*E-mail: fa1sarua@uco.es.

ACKNOWLEDGMENT

A.S. thanks partial support for this work to the Spanish Dirección General de Investigación Cientfica y Técnica (DGICYT) and FEDER under contract FIS2009--07390 and by the Junta de Andalucía.

REFERENCES

(1) Connerade, J.-P.; Dolmatov, V.; Lakshmi, P. *J. Phys. B: At. Mol. Phys.* **2000**, *33*, 251.
(2) Connerade, J.-P.; Semaoune, R. *J. Phys. B: At. Mol. Phys.* **2000**, *33*, 3467.
(3) Dolmatov, V.; Baltenkov, A.; Connerade, J.-P.; Manson, S. *Radiat. Phys. Chem.* **2004**, *70*, 417–433.
(4) Sako, T.; Diercksen, G. *J. Phys. B: At. Mol. Phys.* **2003**, *36*, 1681–1702.
(5) Sarkar, U.; Giri, S.; Chattaraj, P. K. *J. Phys. Chem. A* **2009**, *113*, 10759–10766.
(6) Jaskolski, W. *Phys. Rep.* **1996**, *27*, 1–66.
(7) Cruz, S. In *Advances in Quantum Chemistry*; Sabin, J., Brandas, E., Ed.; Elsevier: San Diego, CA, 2009; Vol. 57; pp 255−283.
(8) Connerade, J.-P.; Kengkan, P. *Idea-Finding Symposium*; EP Systema: Frankfurt, Germany, 2003; pp 35−46.
(9) Hammond, B. L.; Lester, W. A., Jr.; Reynolds, P. J. *Monte Carlo Methods in ab initio Quantum Chemistry*; World Scientific: Singapore, 1994.
(10) Foulkes, W. M. C.; Mitáš, L.; Needs, R. J.; Rajagopal, G. *Rev. Mod. Phys.* **2001**, *73*, 33.
(11) López-Ríos, P.; Ma, A.; Drummond, N.; Towler, M. D.; Needs, R. J. *Phys. Rev. E* **2006**, *74*, 066701.
(12) Parker, W.; Wilkins, J.; Hennig, R. *Phys. Status Solidi B* **2011**, *248*, 267.
(13) Seth, P.; López-Ríos, P.; Needs, R. J. *J. Chem. Phys.* **2011**, *134*, 084105.
(14) Sako, T.; Diercksen, G. *J. Phys.: Condens. Matter* **2005**, *17*, 5159–5178.
(15) Pupyshev, V. I.; Bobrikov, V. *Int. J. Quantum Chem.* **2004**, *100*, 528–538.
(16) Drummond, N.; Towler, M. D.; Needs, R. J. *Phys. Rev. B* **2004**, *70*, 235119.
(17) Buendía, E.; Gálvez, F. J.; Sarsa, A. *Chem. Phys. Lett.* **2008**, *465*, 190–192.
(18) Flores-Riveros, A.; Rodríguez-Contreras, A. *Phys. Lett. A* **2008**, *372*, 6175–6183.
(19) Laughlin, C.; Chu, S.-I. *J. Phys. A: Math. Theor.* **2009**, *42*, 265004.
(20) Le Sech, C.; Banerjee, A. *J. Phys. B: At. Mol. Phys.* **2011**, *44*, 105003.
(21) Banerjee, A.; Kamal, C.; Chowdhury, A. *Phys. Lett. A* **2006**, *350*, 121–125.
(22) Le Sech, C.; Sarsa, A. *Phys. Rev. A* **2001**, *63*, 022501.
(23) Weissbluth, M. *Atoms and Molecules*; Academic Press: San Diego, CA, 1978.
(24) Ludeña, E. *J. Chem. Phys.* **1978**, *69*, 1770–1775.
(25) Yan, Z.-C.; Drake, G. *Phys. Rev. A* **1995**, *52*, 3711–3717.
(26) Gimarc, B. *J. Chem. Phys.* **1967**, *47*, 5110–5115.
(27) Chakravorty, S. J.; Gwaltney, S. R.; Davidson, E. R.; Parpia, F.; Fischer, C. F. *Phys. Rev. A* **1993**, *47*, 3649–3670.
(28) Ralchenko, Y.; Kramida, A. E.; Reader, J. *NIST Atomic Spectra Database*, version 4.0.1; NIST ASD Team: Gaithersburg, MD, 2011. Accessed April 11, 2011.